06

Effect of the activation environment on the thermocatalytic properties of bimetallic nanoparticles on the hexagonal boron nitride surface

© A.S. Konopatsky, V.V. Kalinina, D.V. Barilyuk, D.V. Shtansky

National University of Science and Technology MISiS, Moscow, Russia
E-mail: konopatskiy@misis.ru

Received December 4, 2024
Revised March 12, 2025
Accepted March 13, 2025

This study investigates the effect of activation environment on the catalytic performance of heterogeneous nanostructured catalysts based on FePt bimetallic nanoparticles supported on layered hexagonal boron nitride *h*-BN in carbon monoxide oxidation reactions. The material's structure was characterized by transmission electron microscopy (TEM), scanning transmission electron microscopy (STEM), and energydispersive Xray spectroscopy (EDS) elemental mapping. The surface chemical state of activated samples was analyzed using Xray photoelectron spectroscopy (XPS). The results demonstrate that the choice of activation environment (hydrogen/helium) strongly affects the CO conversion temperature.

Keywords: nanomaterials, catalysis, CO oxidation, activation.

DOI: 10.61011/TPL.2025.06.61291.20212

Since carbon monoxide is one of the main components of many hazardous emissions, the CO oxidation reaction is of great importance both in studying fundamental issues of catalysis where it plays a role of a model reaction [1,2] and in commercially and environmentally significant processes. Achieving high performance in the reaction of thermocatalytic oxidation of CO largely depends on the choice of the catalyst activation mode. A correctly selected activation procedure allows achieving higher CO conversion values, as well as the catalyst stability [3]. In many cases, the catalyst is activated in the hydrogen atmosphere [4].

Hexagonal boron nitride (*h*-BN) has attracted increasing attention as a promising substrate for catalytically active particles. Materials based on it exhibit high performance in many thermocatalytic [5] and photocatalytic processes [6].

It was previously shown that activation of bimetallic FePt nanoparticles on the *h*-BN substrate surface in the hydrogen environment enables achieving 100 % conversion at the temperature of 250 °C [7]. It was noted that activation of FePt/BN in this environment leads to partial chemical ordering in the FePt structure, which may have a positive effect on the CO conversion. In this study we have examined the effect of the FePt/BN activation in inert helium on the material catalytic properties. Particular attention is paid to studying the chemical state of the catalyst surface subjected to various activation modes.

Synthesis of the FePt nanoparticles was performed in the suspension of *h*-BN nanoparticles obtained by ball milling in ethylene glycol. The suspension of *h*-BN nanoparticles was obtained by 10 min ultrasonic dispersion of 200 mg of the *h*-BN powder in 100 ml of ethylene glycol by using a titanium submersible sonotrode with continuous stirring in a magnetic stirrer. After that, the suspension was transferred to a twonecked flask and placed in a flask heater. Under the conditions of lowintensity ultrasonic treatment and continuous blowing of the suspension with an argon flow, the suspension temperature was brought to 170 °C. After that, a solution of chloroplatinic acid, solution of iron (III) chloride with the molar ratio of 1 : 9, and 2 g of NaOH were added to the suspension successively during 2 min. After cooling the synthesis medium to room temperature, the sample was distilled and washed in distilled water in a laboratory centrifuge at the speed of 10 000 rpm.

The obtained material microstructure and elemental distribution was studied by transmission/scanning transmission (TEM/STEM) electron microscopy and energy-dispersive spectroscopy (EDS) using the JEM2100 electron microscope. The surface chemical state was studied by X-ray photoelectron microscopy (XPS) using the AXIS Supra surface analysis instrument for samples activated in a catalytic reactor. After activation and cooling the reactor to room temperature, the samples were transferred to plastic tubes pre-filled with argon, which had screw caps sealed with parafilm in order to reduce the time of samples exposure to air. XPS analysis of the samples was performed after removing them from the reactor.

Activation of the samples, as well as subsequent studying of CO conversion under the oxidation reaction, was performed in a flowthrough quartz reactor. For this purpose, a 50 mg weighed portion of the FePt/BN sample was used. Prior to loading into the reactor, the sample was dispersed with quartz granules of the 200–300 μm fraction up to the total volume of 2 ml. Activation was performed at 500 °C for 4 h in a hydrogen flow, as well as under the same conditions in a helium flow. On the completion of activation and cooling the reactor to room temperature, which took approximately 5 h, the gas flow composition was changed to 5.6 % of CO, 11.1 % of O_2, 83.3 % of He ($43\,200\,\text{ml} \cdot \text{g}_{cat}^{-1} \cdot \text{h}^{-1}$); the gas flowrate was 36 ml/min. Pressure in the reactor was 1 atm. After that, the reactor was

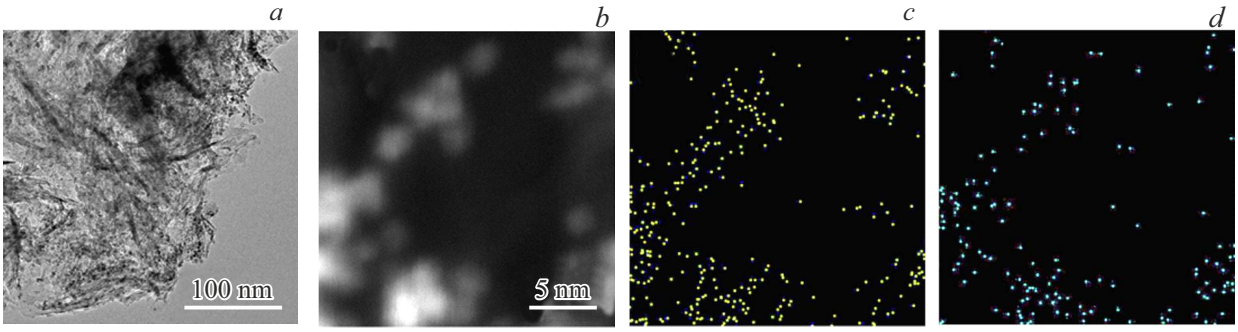

Figure 1. Survey TEM image (a), STEM image (b) and corresponding Fe (c) and Pt (d) elemental distribution maps for the FePt/BN sample.

heated to 300 °C. Heating rate was 2 °C/min in all the cases. The reaction products were studied at different temperatures on mass spectrometer ThermoStar. The carbon monoxide conversion was defined as

$$X = 1 - \frac{Q^f_{\mathrm{CO}}}{Q^s_{\mathrm{CO}}},$$

where Q^s_{CO} is the initial CO flow, Q^f_{CO} is the CO flow at the reactor outlet.

Fig. 1 presents the results of studying the structure of the obtained heterogeneous catalysts FePt/BN. The survey TEM image (Fig. 1, a) shows that the sample is represented by a multitude of thin (typically less than 10 nm thick) and extended (over 100 nm) curved h-BN sheets on which FePt bimetallic nanoparticles are uniformly distributed. This morphology of the h-BN particles is caused by their production procedure, namely, ball milling of powder of micron h-BN particles about 5 μm in average diameter and 200–300 nm in thickness. The structure was analyzed in more details by STEM at a higher magnification (Fig. 1, b). The STEM image shows that average size of the FePt particles is about 2 nm.

Note also that almost all the particles in the image have similar phase contrast, which suggests that they are of the same type. The elemental distribution maps (Fig. 1, c, d) corresponding to the obtained STEM image show that signals from iron and platinum correlate well with each other and, in addition, are consistent with the particle distribution presented in the STEM image. Analysis of the EDS spectrum provided the following chemical composition of the sample (at.%): B — 51.2, N — 44.6, O — 3.6, Fe — 0.3, Pt — 0.3. This allows us to conclude that equiatomic bimetallic FePt nanoparticles were formed on the h-BN powder surface. It is significant that, as shown earlier, synthesis results in formation on the h-BN substrate surface of the bimetallic FePt phase without a considerable amount of the oxide phase [7].

Chemical state of the FePt/BN particle surface after activation in hydrogen and helium was studied by XPS. The most pronounced difference between the samples is observed in the Pt $4f$ spectra (Fig. 2). The Pt $4f$ signal is located at binding energies ranging from 70 to 77 eV and is represented by the typical Pt $4f_{7/2}$ and Pt $4f_{5/2}$ doublet. The main contribution to the signal of each of the activated samples is made by metallic platinum Pt^0. Of interest is a weaker signal located at a higher binding energy. This signal may occur in the Pt $4f$ spectrum in two cases: as a result of the presence of a small amount of oxygen on the particle surface, and as a result of hydrogen adsorption by the particles [8]. In both cases there arises a doublet located in the vicinity of binding energies ~ 77.0 eV (Pt $4f_{7/2}$) and ~ 73.5 eV (Pt $4f_{5/2}$). This peak may be related to both Pt^{2+} and Pt–H. Note that this peak has a low intensity in the sample activated in helium (Fig. 2, a) where its contribution to the total signal is about 15 % and a significantly higher intensity in the sample activated in hydrogen where its contribution is already about 32 % (Fig. 2, b).

To test the assumption that activation in hydrogen leads to its adsorption by FePt nanoparticles on the h-BN surface, an additional activation scheme was selected which employed a higher temperature (800 °C) and time of holding in hydrogen and helium of 1 h. The acquired Pt $4f$ spectra showed that the main contribution to the signal is made, as previously, by Pt^0. However, the peak Pt^{2+} intensity for the sample activated in helium remains virtually unchanged. The share of this component in the total signal (~ 17 %) also remains virtually the same. Thereat, intensity of the signal associated with hydrogen adsorption in the sample activated in H_2 increases significantly; its share amounts to 38 %. Thus, we may conclude that activation of the FePt/BN sample in the H_2 environment leads to hydrogen adsorption on bimetallic particle surfaces (presumably in the atomic form). Due to low content of the active phase and lower XPS sensitivity to iron, a conclusion about the iron chemical state can hardly be drawn. Note that, according to the TEM analysis data, the sample activation initiates a minor agglomeration of FePt nanoparticles whose average size increases, as a result, to 3.2 nm in the sample activated at 500 °C and to 4.5 nm in the sample activated at 800 °C. As the EDS analysis has shown, chemical composition of the samples do not change as a result of activation.

The results of catalytic tests of samples activated both in hydrogen and helium are presented in Fig. 3. The obtained

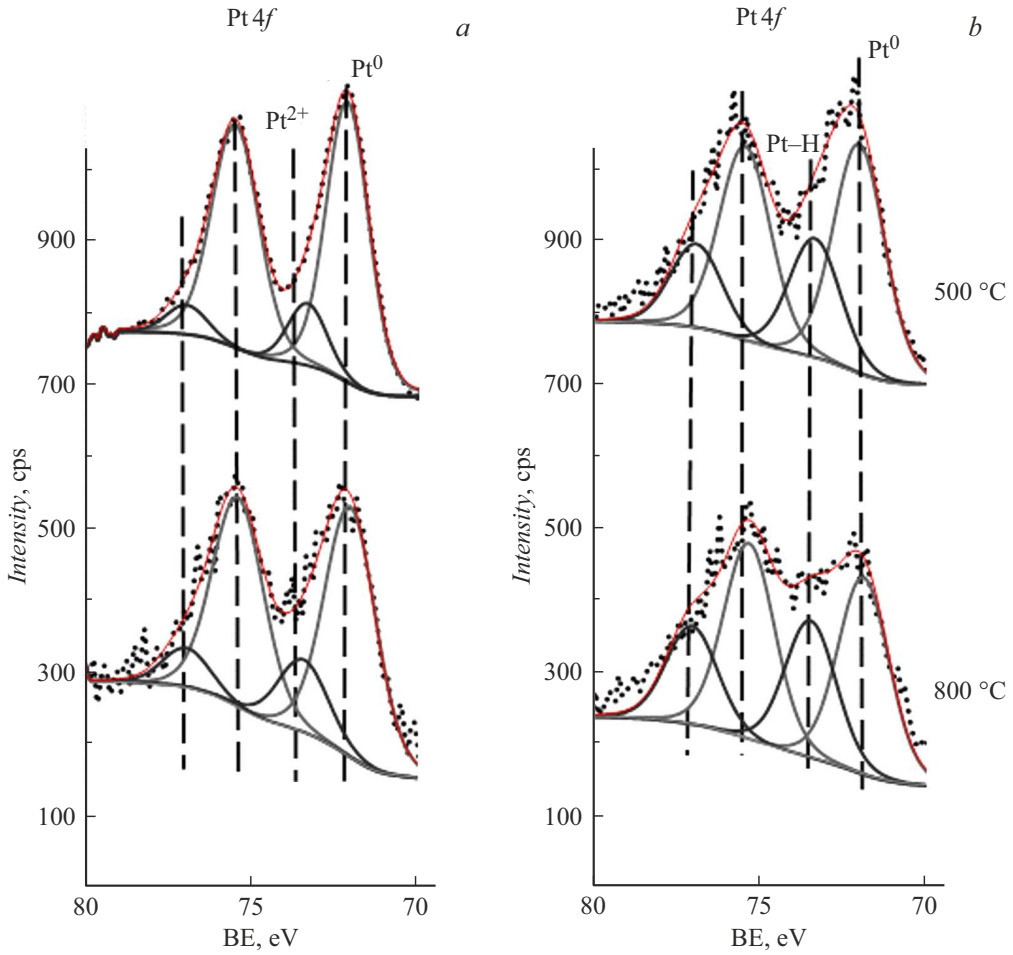

Figure 2. XPS spectra of Pt 4*f* for the FePt/BN sample activated at different temperatures in the helium (*a*) and hydrogen (*b*) environments.

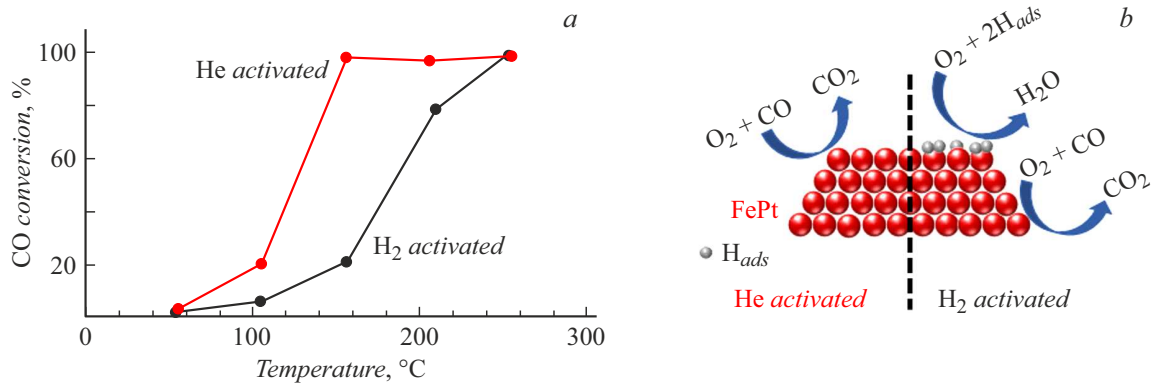

Figure 3. *a* — CO conversion on samples activated at 500 °C for 4 h in hydrogen and helium versus the test temperature; *b* — schematic representation of the reaction in different activation environments.

testtemperature dependences of the CO conversion value show that the sample activated in helium reaches 100 % conversion of carbon monoxide already at 156 °C, which is a very high result for catalysts lowloaded (less than 1 at.%) with the catalytically active phase. At the same time, the sample exhibits a considerable activity (20 % CO conversion) already at temperatures close to 100 °C. Thus, the obtained material may be classified as a lowtemperature catalyst for the carbon monoxide oxidation [9].

A different situation is observed for the sample activated in hydrogen. The complete conversion of CO is achievable at a considerably higher temperature (253 °C), while conversion at low temperatures is insignificant and does not exceed 5 %. The reason for such a variation in the material

catalytic properties may be associated with adsorption of a significant amount of hydrogen on the surface of catalytically active nanoparticles. It is possible to assume that in this case the dissociative hydrogen adsorption takes place on the FePt nanoparticle surface. Presumably, dissociation proceeds at the platinum centers. Besides, it cannot be ruled out that emerging atomic hydrogen penetrates into the FePt nanoparticle lattice. In the course of the catalytic test, the H_2 desorption at low temperatures is still not sufficiently intense, due to which active centers remain occupied by hydrogen thus being inaccessible to CO and O_2. At higher temperatures, when the catalystś efficiency increases, what actually takes place is not the pure CO oxidation reaction but the so-called PROX reaction, i. e. reaction of selective CO oxidation in the presence of hydrogen as a reducing agent [10]. In this case, a portion of oxygen supplied to the reactor is spent not on the CO oxidation according to reaction $CO + (1/2)O_2 \rightarrow CO_2$, but on reaction $2H_{ads} + (1/2)O_2 \rightarrow H_2O$ (Fig. 3, *b*). Importantly, hydrogen may be not only on the surface of FePt nanoparticles but also inside their structure (as mentioned above) and, in addition, inside the *h*-BN substrate structure where it can get by the spillover mechanism. In this case, the *h*-BN substrate characterized by a high adsorption capacity for hydrogen plays the role of a source of hydrogen in the reaction zone. It may also be assumed that hydrogen adsorbed on platinum can interact with oxygen in the reaction mixture, which leads to formation of water and chemical adsorption of its molecules on platinum centers; this may also explain the observed reduction of catalytic properties of the sample activated in hydrogen.

Emphasize that the proposed process may be classified as the PROX reaction only conditionally, since hydrogen was not supplied to the reactor intentionally; its presence was caused only by adsorption on the FePt particle surface at the stage of activation. Along with this, the PROX reaction is also of great industrial importance in view of the technique for hydrogen purification from CO, which is in demand in the field of developing fuel cells.

Thus, our study has shown that environment for the FePt/BN activation significantly affects the material catalytic performance in the CO oxidation reaction. A higher CO conversion may be achieved in the case of activating the material in helium. It has been also established that FePt/BN is a promising material for the process of selective CO oxidation.

Funding

The study was supported by the Russian Science Foundation (project № 20-79-10286-P).

Conflict of interests

The authors declare that they have no conflict of interests.

References

[1] F. Doherty, H. Wang, M. Yang, B.R. Goldsmith, Catal. Sci. Technol., **10**, 5772 (2020). DOI: 10.1039/D0CY01316A
[2] N.K. Soliman, J. Mater. Res. Technol., **8**, 2395 (2019). DOI: 10.1016/j.jmrt.2018.12.012
[3] J.H. Yang, J.D. Henao, M.C. Raphulu, Y. Wang, T. Caputo, A.J. Groszek, M.C. Kung, M.S. Scurrell, J.T. Miller, H.H. Kung, J. Phys. Chem. B, **109**, 10319 (2005). DOI: 10.1021/jp050818c
[4] S. Xie, Y. Lu, K. Ye, W. Tan, S. Cao, C. Wang, D. Kim, X. Zhang, J. Loukusa, Y. Li, Y. Zhang, L. Ma, S.N. Ehrlich, N.S. Marinkovic, J. Deng, M. Flytzani-Stephanopoulos, F. Liu, Environ. Sci. Technol., **58**, 12731 (2024). DOI: 10.1021/acs.est.4c03078
[5] A.S. Konopatsky, D.V. Leybo, K.L. Firestein, I.V. Chepkasov, Z.I. Popov, E.S. Permyakova, I.N. Volkov, A.M. Kovalskii, A.T. Matveev, D.V. Shtansky, D.V. Golberg, ChemCatChem, **12**, 1691 (2020). DOI: 10.1002/cctc.201902257
[6] X. Li, J. Zhang, S. Zhang, S. Xu, X. Wu, J. Chang, Z. He, J. Alloys Compd., **864**, 158153 (2021). DOI: 10.1016/j.jallcom.2020.158153
[7] A.S. Konopatskii, K.L. Firestein, I.N. Volkov, D.V. Leibo, V.V. Kalinina, D.V. Golberg, D.V. Shtanskii, Tech. Phys. Lett., **47**, 792 (2021). DOI: 10.1134/S1063785021080186.
[8] K.A. Stoerzinger, M. Favaro, P.N. Ross, J. Yano, Z. Liu, Z. Hussain, E.J. Crumlin, J. Phys. Chem. B, **122**, 864 (2018). DOI: 10.1021/acs.jpcb.7b06953
[9] R.M. Al Soubaihi, K.M. Saoud, J. Dutta, Catalysts, **8**, 660 (2018). DOI: 10.3390/catal8120660
[10] K. Liu, A. Wang, T. Zhang, ACS Catal., **2**, 1165 (2012). DOI: 10.1021/cs200418w

Translated by EgoTranslating